

# Body composition analysis of the pig by magnetic resonance imaging<sup>1</sup>

A. D. Mitchell<sup>\*,2</sup>, A. M. Scholz<sup>†</sup>, P. C. Wang<sup>‡</sup>, and H. Song<sup>‡3</sup>

<sup>\*</sup>USDA, ARS, Beltsville, MD 20705; <sup>†</sup>Ludwig-Maximilians University Munich, 85764 Oberschleissheim, Germany; and <sup>‡</sup>Howard University, Washington, DC 20007

**ABSTRACT:** Magnetic resonance imaging (MRI) was used to measure, in vivo, the volume of several organs and tissues of a total of 111 pigs (males and females) ranging in BW from 6.1 to 97.2 kg. In one experiment the in vivo MRI volumes were compared to tissue or organ weights obtained by dissection. For internal organs, the correlation ( $R^2$ ) between MRI volume and dissected weight ranged from 0.64 (SE of estimation = 65 g) for the heart to 0.90 (SE of estimation = 125 g) for the liver. The MRI volume of the kidneys was approximately 10% less than the dissected weight, whereas the MRI volumes of the heart, liver, and brain exceeded the weights of dissected organs by 13, 17, and 26%, respectively. For fat and muscle tissues, the correlation between MRI volume and dissected weight ranged from 0.82 (psoas muscle) to 0.97 (total right ham muscles). The MRI volume of the backfat and shoulder muscles exceeded the dissected weights by approximately 2%, whereas the MRI volumes of the ham muscles, jowl fat, longissimus muscle, and psoas muscle

were 2, 8, 18 and 20% less than their respective weights. In another series of experiments, MRI volume measurements of fat and muscle regions (jowl fat, backfat, shoulder muscles, LD muscles, psoas muscles, ham muscles, a 10-cm section of the longissimus muscles and overlying fat, and a 15-cm section of the ham muscles and overlying fat) were evaluated by stepwise regression for the prediction of total body fat, lean, and protein. The best prediction of percentage total body fat was obtained using the fat volume from the 10-cm section of longissimus muscle and the fat:muscle ratio from the 15-cm section of the ham ( $R^2 = 0.9$ ). The best prediction of percentage total body protein was obtained using a combination of the volumes (as a percentage of BW) of jowl fat, backfat, shoulder muscle, and ham muscle ( $R^2 = 0.62$ ). The combination fat volume from the 10-cm section of longissimus muscle, the fat:muscle ratio from the 15-cm section of the ham, and the lean volume percentage from the 15-cm section of ham provided the best prediction of the percentage of total body lean ( $R^2 = 0.88$ ).

Key Words: Body Composition, Magnetic Resonance Imaging, Pigs

©2001 American Society of Animal Science. All rights reserved.

J. Anim. Sci. 2001. 79:1800–1813

## Introduction

Magnetic resonance imaging (MRI) is widely recognized as one of the most powerful diagnostic tools of modern medicine. The MR image is based on the magnetic resonant properties of protons associated with water and lipid molecules of tissues and results in a range of signal intensities capable of distinguishing numerous tissues and organs, including fat and muscle. A series

of consecutive images can be reconstructed to render a volume measurement of the region of interest. Body composition measurements can consist of volume measurements of a specific tissue (i.e., muscle or group of muscles, adipose tissue depots) in total or from a defined region.

In studies in which in vivo MRI volume measurements have been compared with the weights of the dissected tissues,  $R^2$  values have ranged from 0.48 to 0.98 (Mitchell et al., 1991b; Fowler et al., 1992; Kallweit et al., 1994). The accuracy of the volume measurement by MRI is primarily a function of edge detection or tissue separation (signal intensity classification) and the relationship between slice thickness and total volume of the region of interest. Due to the practical limitations of total body analysis, the prediction of body composition based on MRI analysis relies on the volume measurements of specific regions of muscle and adipose tissue. A study by Baulain et al. (1996), using MRI to measure the fat and lean of five body regions of 143

<sup>1</sup>Mention of a trade name does not constitute a guarantee or warranty by the USDA and does not imply its approval to the exclusion of other products that may be suitable.

<sup>2</sup>Correspondence: Bldg. 200, Rm. 205, BARC-East (fax: 301-504-8623; E-mail: mitchell@anri.barc.usda.gov).

<sup>3</sup>Present address: Shenzhen Mindt Instruments Co., Ltd., R1-B1, Shenzhen Hi-Tech Industrial Park, Shennan Ave., Shenzhen 518057, China.

Received October 12, 2000.

Accepted March 26, 2001.

pigs, reported prediction equations with excellent coefficients of determination for total ( $R^2 \geq 0.9$ ) and percentage ( $R^2 \geq 0.8$ ) fat and lean content of the dissected carcass. Thus, it is important to determine which region(s) will correlate best with total body composition. The purpose of the present study was to validate MRI tissue volume measurements within the pig and to compare regional and total body MRI approaches to estimating total body fat and lean content.

### Methods and Materials

Magnetic resonance imaging was performed on a total of 111 pigs (intact males and females, 6.1 to 97.2 kg) in four separate experiments. In Exp. 1 (28 pigs), the MRI volume measurements of body regions and internal organs were compared with dissected weights. In Exp. 2 (22 pigs), MRI volume measurements of fat and muscle regions were evaluated for predicting total carcass composition based on chemical analysis of the ground carcass. In Exp. 3 (46 pigs), MRI volume of a 10-cm section of the longissimus muscle and overlying fat and the volume of a 15-cm section of the ham muscle and its overlying fat were used to predict carcass composition. In Exp. 4 (15 pigs), MRI volume of only a 2.45-cm section of the longissimus muscle and overlying fat was used for prediction of carcass composition. These studies were conducted in accordance with protocols approved by the USDA-ARS, Beltsville Animal Care and Use committee.

**Magnetic Resonance Imaging.** The magnetic resonance (MR) spectroscopic signal is produced by placing the sample in a static magnetic field and exciting it with radiofrequency (RF) waves at the resonant frequency determined by the magnetic field strength and the nucleus to be studied. After excitation, the sample emits a RF signal that can be detected by a coil placed around the sample. The intensity of the emitted signal is related to the number of protons present in a given volume. The intensity also depends on the spin-lattice ( $T_1$ ) and the spin-spin relaxation times ( $T_2$ ) of the excited sample. The  $T_1$  values, as measured in a 1.5 T MRI instrument, are about 260 ms for fat and in the range of 500 to 920 ms for various nonfatty tissues, including skeletal muscle (900) (Bottomley et al., 1984). The  $T_2$  relaxation time for muscle is 44 ms; for subcutaneous adipose tissue it is 130 ms.

Differences in the MR behavior of water and lipid protons result in signals that can be resolved in a frequency spectrum. The MR image is generated by imposing gradient magnetic field conditions upon the sample during the excitation and recovery periods to establish spatial encoding (the unique relationship between frequency and location for all volume elements of the object) (Stark and Bradley, 1999). Differences in the water proton content and the MR relaxation times of tissues permit excellent contrast between fat, muscle, and other soft tissues. For the commonly used spin-echo imaging technique, the image contrast is primarily due

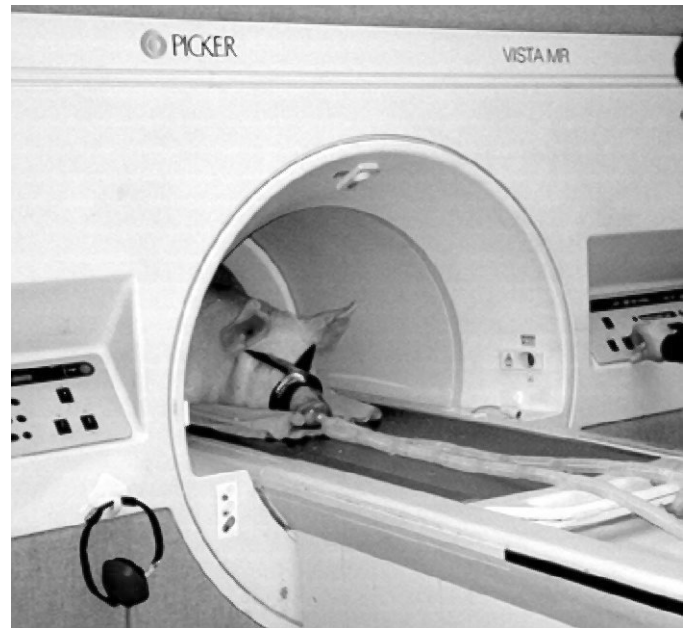


**Figure 1.** Position of a pig in the Picker 1.5 T tomograph for Exp. 1, 2, and 3 (mask attached to the pig was used to control the breathing function under anesthesia, Exp. 3).

to the differences in  $T_1$  and  $T_2$  relaxation times of the adjacent tissues. The difference in the percentage of water content for different tissues is not as important as the  $T_1$  and  $T_2$  relaxation times. In the spin-echo image technique, only the free water (i.e., water not bound to the large molecules) contributes to the signal.

The pigs in Exp. 1 and 2 were killed by pentobarbital injection prior to scanning, whereas the pigs in Exp. 3 and 4 were first sedated by i.m. injection of a mixture of ketamine, Telazol, and xylazine then maintained under anesthesia (isoflurane) during the scanning procedure. A series of cross-sectional images was obtained using a Picker Vista (Picker International, Highland Heights, OH) whole-body (1-m bore diameter) imaging system operated at 1.5 T (63 MHz) in Exp. 1, 2, and 3 (Figure 1). In Exp. 4, a total of five images were obtained using a saddle-shaped surface coil placed on the back of the pig in a Varian horizontal (0.3-m bore diameter) MR spectroscopy/imaging system (Varian, Palo Alto, CA) operated at 4.7 T (200 MHz) (Scholz et al., 1995). Each pig was placed in the instrument(s) in a prone position. Scouting images in the sagittal plane were used to verify location and orientation. A multi-slice, spin-echo imaging technique was performed using an echo time of 20 ms and a recovery time of 1.3 s (400 ms in Exp. 4) with two-signal averaging (four-signal averaging in Exp. 4). Each image had a slice thickness of 10 mm (4.9 mm in Exp. 4), with no gap between images. Total body scans were performed on pigs in Exp. 1 and 2. In Exp. 3 and 4, only the trunk (and back legs, Exp. 3) were scanned.

**Image Analysis.** Images obtained from Exp. 1 and 2 (50 pigs, 8.5 to 60.5 kg) were analyzed for quantification

of the MRI volumes of specific muscle regions, adipose tissue regions, or organs. The outline of areas within each cross-section was traced from the image on x-ray film transparencies using a translucent tablet and digitizing puck. The image tracings were processed and volume measurements performed using PC3D, a three-dimensional reconstruction program (Jandel Scientific, San Rafael, CA). In both Exp. 1 and 2, volumetric analysis of the total body and the following regions was performed: jowl fat, back fat, left and right shoulder muscles, left and right longissimus muscles, left and right psoas muscles (combined), and left and right ham muscles (Figure 2). In addition, in Exp. 1, the following internal organs were also measured: brain, heart, liver, and left and right kidneys.

For the second group of 61 pigs (6.1 to 15.0 and 26.4 to 97.2 kg, Exp. 4 and 3, respectively), MRI volumes of fat and muscle within specific regions of the back (10

cm or 2.45 cm) and ham (15 cm) were compared with chemical analysis. These images were processed using Analyze software (version 6.0, Mayo Foundation, Rochester, MN), using on-screen tracing techniques. The volume of both longissimus muscles and of the overlying fat was measured in a 10-cm section (2.45-cm section, Exp. 4) (Scholz et al., 1995) starting at the 14th vertebra in the cranial direction, and the volume of the ham and its overlying fat was determined in a 15-cm section in the cranial direction, starting at the base of the tail (Figure 3). Because the tracing of the muscle areas of the ham included bone and connective tissue as well as muscle, it is hereafter referred to as "lean" rather than muscle. In order to harmonize Exp. 3 and 4, the volume measured from the 2.45-cm section in Exp. 4 was adjusted to a 10-cm section using the equation  $\text{Volume (10 cm calculated)} = \text{volume (2.45-cm section)} \times (10/2.45)$ . No correction factor was applied for individual variation in muscle and fat area changes (decrease or increase) from the 14th to 12th vertebrae. Generally, the muscle and overlying fat area slightly decreased from the 14th vertebra in the cranial direction. Due to anatomical restrictions, the surface coil could not be used effectively above the hind leg region in Exp. 4.

**Carcass Analysis.** After imaging, the pigs were dissected by removing the head and internal organs. The remainder of the carcass was either dissected into areas of fat and muscle corresponding to image analysis (Exp. 1) or ground and analyzed for lipid, protein, and water content (Exp. 2, 3, and 4). Lipid analysis was performed by chloroform-methanol extraction (Folch et al., 1957), protein by Kjeldahl nitrogen determination, and water content by lyophilization.

**Statistical Analysis.** Male and female pigs were grouped together for statistical analysis. In order to quantify the accuracy of the carcass composition estimation by magnetic resonance volume measurements, coefficients of determination ( $R^2$ ) and standard errors of estimation ( $\text{SEE} = \sqrt{\text{MSE}} = \text{root mean square error from variance analysis}$ ) were calculated for single and multiple regression equations using the SAS statistical package (Version 6; SAS Inst. Inc., Cary, NC). A stepwise regression procedure with a significance level of  $P = 0.05$  for variables entering and staying in the equation was used to calculate the best-fitting (multiple) regression equations.

## Results

### Tissue and Organ Volume Measurements

Typical cross-sectional MR images of the pig are shown in Figure 4. These images illustrate some of the various tissues that can be observed in the MR image, with particular reference to the excellent contrast between fat and muscle tissue. The results of Exp. 1, in which MRI volume analysis was compared directly to the weights of dissected tissues and organs, are shown in Table 1. By imaging of the entire span of the body

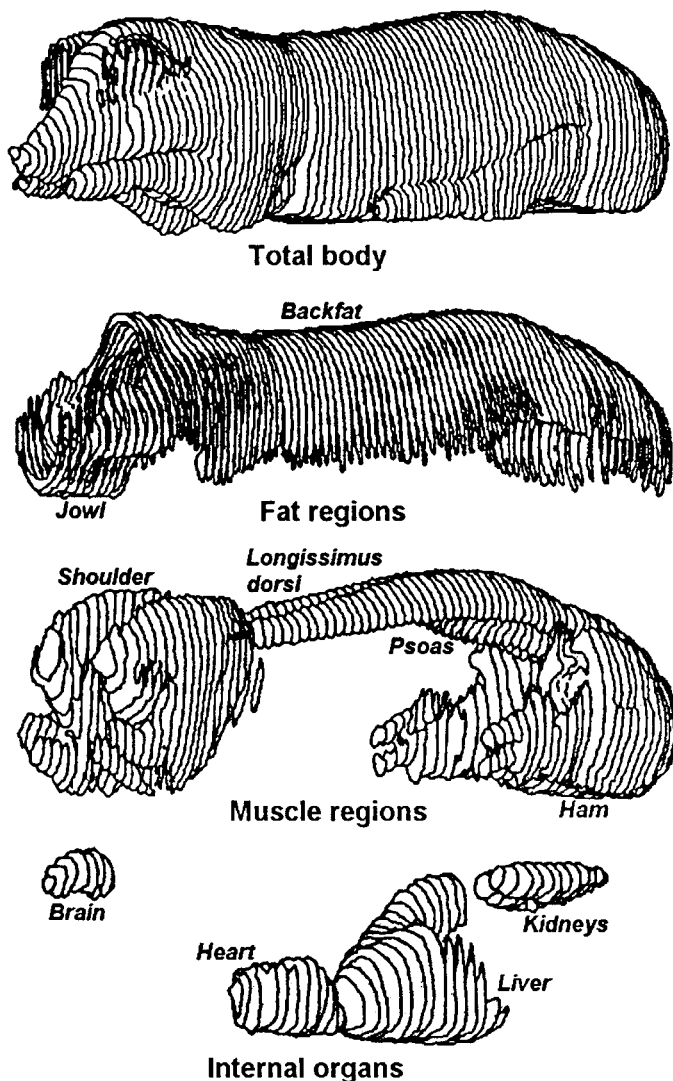


**Figure 2.** Reconstruction of image tracings of total body, fat regions (jowl and back fat), muscle regions (shoulder, longissimus, psoas, and ham), and internal organs (brain, heart, liver, and kidneys) of a pig.

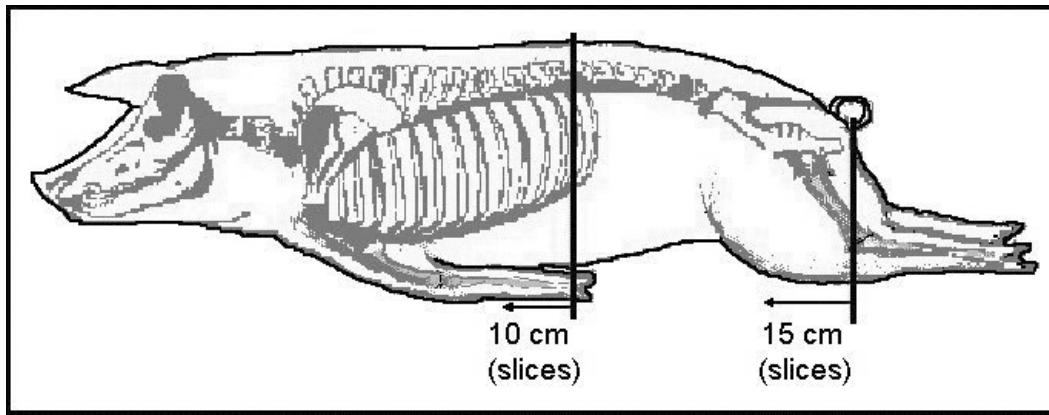


**Figure 3.** Location of regions analyzed to measure loin and ham magnetic resonance image volumes in swine.

it is possible to measure total body volume; this provides an additional level of validation for the technique. The time required to scan the entire pig ranged from about 24 to 60 min, depending on the size of the pig and the specific MR imaging technique. A reconstructed outline from MRI tracings of the body of a pig is shown in Figure 2.

Within the body four distinct muscles or groups of muscles were traced from the cross-sectional images. These consisted of the shoulder/arm muscles, the longissimus muscle, the psoas muscle, and the leg or ham muscles. Except for the psoas muscle, the right and left sides were analyzed separately. A reconstruction of the MRI tracings of these muscle areas is shown in Figure 2. Because of the close association of the shoulder muscles with the underlying neck muscles, this was the most difficult muscle region to trace and dissect. The mean values for MRI volume measurement of the total body and larger areas, including the ham muscles, shoulder muscles, and back fat, were all within  $\pm 2.8\%$  of the dissected weight. The best agreement between weight and volume measurement was obtained with ham muscles. A plot of the relationship between weight and volume measurements is shown in Figure 5. Volume measurements of both the longissimus and psoas muscles were approximately 20% less than the weights of the dissected muscles, which may be the result of discrepancies between the boundary of the muscles as dissected and traced. However, both were highly correlated ( $R^2 = 0.93$  and  $0.82$ , longissimus and psoas, respectively).

Because the subcutaneous fat is the major fat depot in the pig, the back fat and jowl regions were chosen for measurement by dissection and MRI volume analysis (Figure 2). A substantial amount of fat is also found in the abdominal region; however, this fat is interspersed with muscle, making it difficult to dissect and trace from the images. The MRI volume measurement of back fat was in close agreement and highly correlated with the corresponding weight measurement obtained by dissection. The relationship between MRI volumes and dissected weights for jowl and back fat is shown in Figure 5.

The MRI volume and weight measurements were made for the brain, heart, liver, and kidneys (Figure 2). The highest correlation coefficients were observed for the liver and kidneys, and the best agreement between weight and volume was observed for the heart and kidneys. The MRI volume measurement of the kidneys was about 10% less than the dissected weight. However, the MRI volume measurements of the heart, liver, and brain exceeded the weights by 13, 17, and 26%, respectively. Figure 5 shows the relationship between MRI volumes and dissected weights of internal organs.

#### *Prediction of Total Body Composition*

From the series of total-body MRI scans (Exp. 2), volumetric analysis was performed on two regions of subcutaneous fat (jowl and back fat) and four muscle regions (shoulder, longissimus, psoas, and ham muscles). Using regression analysis, these individual regions were evaluated for prediction of total body fat, lean, and protein content (Table 2). The MRI volume-percentage (the volume of a region expressed as a percentage of total body volume) of each region was compared with percentages of fat, lean (water plus protein), and protein obtained by chemical analysis. Likewise, the MRI volume ( $\text{cm}^3$ ) was compared with weights of fat, lean, and protein obtained by chemical analysis. In addition, the fat-muscle ratio (ratio of the total volume of fat regions to total volume of muscle regions) was compared to both the percentages and weights of fat, lean, and protein. The MRI volume measurement for back fat gave the highest correlation with percentages of fat (0.783), lean (0.725), and total weight of fat (0.952). The MRI volumes of shoulder, longissimus, and ham muscles gave the highest correlation with total weights of lean (0.964 to 0.981) and protein (0.903 to 0.939). None of the volume measurements was highly correlated with the percentage of protein, although the fat:muscle ratio (0.224) was higher than the other measurements.

The relationship between the observed quantities of fat, lean, and protein and the quantities predicted based

on MRI volumetric analysis is shown in Figure 6. The multiple regression equations used for obtaining the predicted values were generated from the data of Exp. 2 and are as follows:

$$\text{Fat (g)} = -231.4 - 1.252 \times \text{JF} + 1.38 \times \text{BF} + 0.96 \times$$

SM

$$\text{Lean (g)} = 4,331 + 0.906 \times \text{BF} + 3.294 \times \text{SM} + 4.511 \times \text{LDM}$$

$$\text{Protein (g)} = 240.6 - 1.221 \times \text{JF} + 0.257 \times \text{BF} + 0.927 \times \text{SM} + 10.367 \times \text{PM}$$

In these equations, the MRI volumes of jowl fat (**JF**), back fat (**BF**), shoulder muscle (**SM**), longissimus muscle (**LDM**), and psoas muscle (**PM**) are expressed as cubic centimeters.

Another approach to predicting body composition involved imaging specifically defined sections of the body in vivo (Figure 3). From Exp. 3 and 4, the relationship between total body composition and the MRI volumes or MRI volume portions of sections of the longissimus muscle (Exp. 3 and 4) and ham lean tissue (only Exp. 3) and their overlying fat was determined (Tables 3, 4, and 5). The MRI volume portion is defined as section measurement adjusted to the actual BW in cubic centimeters per kilogram BW. In Exp. 3 and 4 analyzed separately, analogous to Exp. 2, the highest correlation with carcass fat percentage was achieved using the MRI back fat volume portion (longissimus fat portion,  $\text{cm}^3/\text{kg BW}$ ) and the fat:muscle ratio of the loin section, whereas carcass lean percentage correlated highest with the ham-lean portion and the fat:muscle ratio of the loin section. As in Exp. 2, the MRI volumes of ham lean tissue, followed by the volume of the longissimus muscles, resulted in the highest correlation with total lean (g) and protein (g), whereas the corresponding fat layers correlated highest with total fat (g). Again, none of the volume measurements was highly correlated with the percentage of protein, although the fat:muscle ratio in the loin region showed a slightly higher relationship than the other measurements.

Analyzing Exp. 3 and 4 together (3 + 4) by considering only the shared traits of the loin region leads to slightly different results for the relationship between the longissimus muscle portion and carcass fat percentage or carcass lean percentage. Both correlations were higher than those of the two separate experiments consisting of different weight groups (6.1 to 15 kg and 26.4 to 97.2 kg), due to a changed pattern in the variation for the whole weight range. The change in carcass composition (based on chemical analysis) over the range of 6.1 to 97.2 kg live BW for the pigs included in Exp. 3 and 4 is shown in Figure 7. Most dramatic was the drop in water content from approximately 69% to approximately 55% and the increase in lipid content from approximately 11% to 26%. At the same time the protein content increased slightly from less than 16% to 18%, where it remained relatively constant. The MRI analysis of the volumes of fat and muscle for the loin region of the same group of pigs is shown in Figure 8. These results indicate a linear increase in muscle volume, a curvilinear increase in fat volume, and concave pattern for the fat:muscle ratio.

From Exp. 2, 3, 4, and 3 + 4 stepwise regression analysis was used to select the best model for prediction

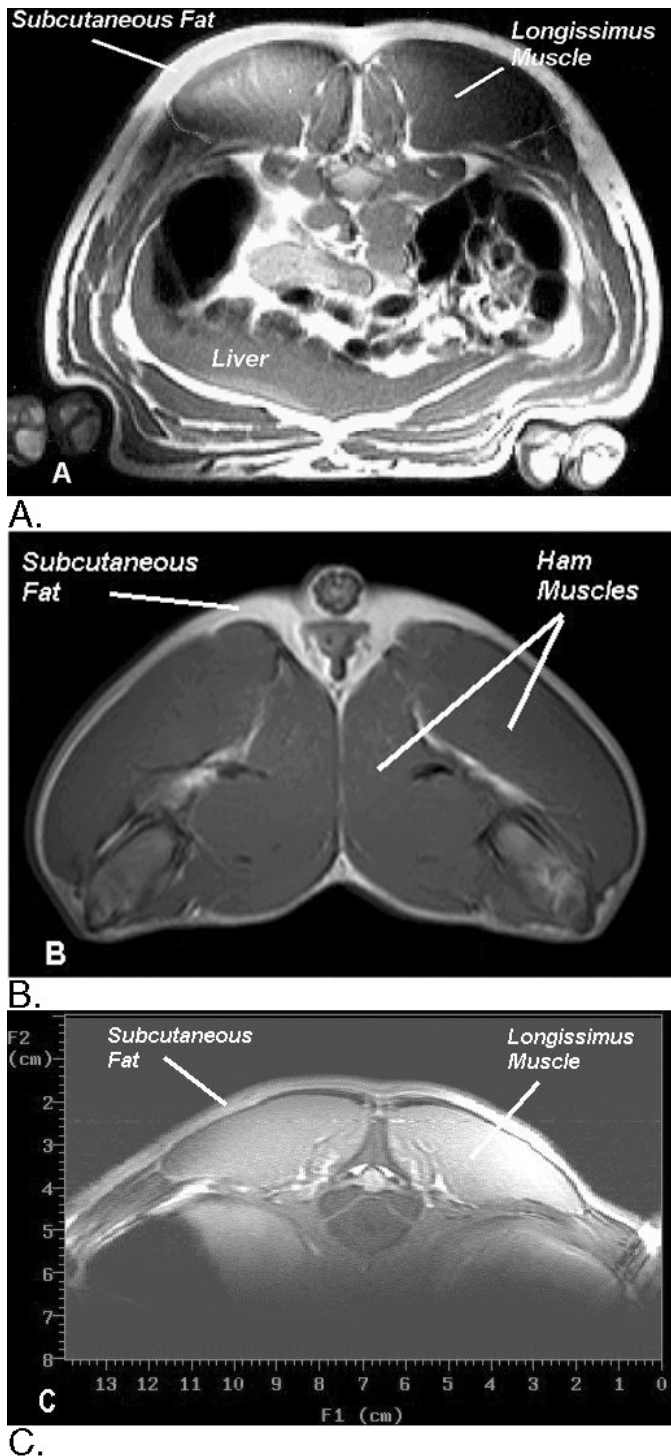


**Figure 4.** Cross-sectional magnetic resonance images (MRI) taken through the abdominal (A) and ham (B) regions of a pig using the Picker 1.5 T whole body system and a typical image of the loin region (C) of a pig using the surface coil in the Varian 4.7 T system.

**Table 1.** Relationship between magnetic resonance imaging (MRI) volume analysis and dissected weights of various tissues and organs from male and female pigs from Exp. 1

Organ or tissue <sup>a</sup>	Dissected weight, g	MRI volume, cm <sup>3</sup>	R <sup>2</sup>	SEE <sup>b</sup>
Jowl fat	403 ± 269 <sup>c</sup>	371 ± 213 <sup>c</sup>	0.87	99
Back fat	2,681 ± 1,788	2,733 ± 1,837	0.94	418
L shoulder muscle	1,254 ± 606	1,288 ± 649	0.87	222
R shoulder muscle	1,254 ± 621	1,276 ± 630	0.83	261
L longissimus muscle	796 ± 432	660 ± 379	0.93	109
R longissimus muscle	822 ± 458	659 ± 384	0.93	126
L and R psoas muscle	268 ± 127	214 ± 116	0.82	55
L ham muscle	2,377 ± 1,173	2,346 ± 1,207	0.96	224
R ham muscle	2,389 ± 1,192	2,323 ± 1,189	0.97	194
Brain	79 ± 14	100 ± 19 <sup>***</sup>	0.67	8
Heart	270 ± 107	306 ± 114	0.64	65
Liver	1,100 ± 383	1,286 ± 298	0.90	125
L kidney	98 ± 40	87 ± 36	0.84	17
R kidney	99 ± 39	90 ± 39	0.86	15
Whole body	37,592 ± 17,829	36,526 ± 18,003	0.99	1,610

<sup>a</sup>Left and right are designated by L and R.

<sup>b</sup>Standard error of estimate.

<sup>c</sup>Mean ± SD, n = 28.

<sup>\*\*\*</sup>MRI volume significantly different from dissected weight at  $P < 0.001$ .

of percentages of carcass lipid, protein, and lean. These results are shown in Table 6. For carcass lipid and lean percentages, the combination of longissimus fat volume and longissimus muscle volume portion (cm<sup>3</sup>/kg BW) from Exp. 3 + 4 and the combination of longissimus fat volume, ham fat:muscle ratio, and ham lean volume portion (only for carcass lean percentage) from Exp. 3 gave similar results that were both better than those from models selected from Exp. 2 and 4. Experiments 2 and 4 covered smaller weight ranges than Exp. 3 and 3 + 4. Experiment 4 included pigs ranging only from 6.1 to 15 kg BW. However, the combination of fat and muscle volumes (jowl fat volume percentage, back fat volume percentage, shoulder muscle volume percentage, and ham muscle volume percentage) from Exp. 2 provided the best estimate for the percentage of carcass protein.

## Discussion

Similar to x-ray computer tomography (CT) and ultrasound imaging, MRI is a measurement system designed to quantify components at the tissue-system level of body composition, describing the anatomical distribution of body tissues in vivo in swine (Foster and Fowler, 1988; Fuller et al., 1994; Baulain and Scholz, 1996) and humans (Elbers et al., 1997; Heymsfield et al., 1997). The differences in concentration, mobility, and relaxation properties of the hydrogen nuclei in different tissues result in a variation of image signal intensities (gray values). Although some of the early MRI studies of human body composition used an inversion recovery imaging sequence (Fuller et al., 1987; Seidell et al., 1990), the spin-echo sequence, as used in the present study, with echo times of 17 to 50 ms and recovery times of 210 to 780 ms, has been used in more recent

studies (Møller et al., 1994; Lee et al., 2000; Morais et al., 2000).

Different approaches can be used to process the images and statistically analyze the signal intensity information in order to quantify tissue volumes. In most cases, a “knowledge-based” region or volume of interest must first be defined. This can be done manually, semi-automatically, or, in the best case, fully automatically using line-drawing software. The volume calculation can be performed by counting the number of pixels that represent either fat, muscle, or bone tissue, converting the numbers into area measurements, and then multiplying the area(s) by the slice thickness to obtain the tissue volumes. In addition to the manual tracing techniques applied in these studies, image segmentation can be accomplished by automated procedures: 1) active contouring of the region or line drawing, 2) a histogram-based thresholding segmentation, and 3) a two-dimensional/three-dimensional region growing method. These automated procedures and their application to body composition analysis of rats and mice was illustrated by Tang et al. (2000). A fourth automated procedure was developed by Scholz et al. (1993), applying a cluster analysis to divide the complete region of interest into a specific number of tissue classes (e.g., fat and muscle).

Inhomogeneity of the magnetic field or a nonuniform RF coil response requires correction of the image intensity. The effects of inhomogeneity can be seen in Figure 4, in which some areas of fat and lean appear darker than others. Simple attempts at minimizing this effect using magnitude images can result in an “absolute value” artifact, in which signals from high-fat voxels (volume elements) can be misinterpreted as a water signal (Kaldoudi and Williams, 1992). Phase-correction algorithms have been proposed to correct for regional

field inhomogeneities (Yeung and Kormos, 1986; Borrello et al., 1987; Glover and Schneider, 1991). If extensive correction is necessary, then it is probably more expedient and accurate to resort to manual tracing. Line drawing (with an on-screen cursor) is controlled either completely by the operator, depending on his/her anatomical knowledge, or partly by the software, depending on threshold settings based on signal intensity differences. In that way the operator controls the

exact anatomical definition of the tissue-related regions (volumes) of interest.

The computer-based regional growth or “seed-growing” procedures draw a region starting from an initial location in the tissue of interest and gradually expand to cover all the tissue represented by pixels. This technique provides an error source when the tissue of interest is merged with another tissue of the same signal intensity range on the screen (e.g., two different muscles or different visceral fat layers) or is scattered over the image (Elbers et al., 1997).

The histogram analysis, extended to a contour-following algorithm by noise correction, uses the signal intensity frequency histogram of an image (slice) and dynamic threshold intensities to separate the pixels into different tissue classes (Thomas et al., 1998). Problems arise through pixels that contain, for example, both fat and muscle tissue. For the histogram analysis, a stepwise regression method can be applied on the large number of potential regression variables (signal intensity classes) in order to reduce the number of variables for the prediction of body composition. However, this method lacks robustness. Derived equations for one set of data may not apply to another set of data within the same population or, especially, another population (Szabo et al., 1999). Another approach in the use of frequency data involves evaluating the image by fitting a “mixture distribution,” described by Luiting et al. (1995) for CT data, which calculates, besides the two normal distributions for fat and muscle tissue, a third normal distribution for combined tissues. This information can be used to compute the proportion of tissues and, finally, tissue volumes.

The gray value (signal intensity) distribution within an MR image can also be used to perform a cluster analysis. In the first step of image processing, regions of interest have to be drawn to exclude those parts that do not contribute to lean and fat. In the next step the masked images are analyzed by means of a disjoint cluster analysis on the basis of the Euclidean distances computed from one or more variables (Scholz et al., 1993). These variables may be specific MR parameters such as proton density and relaxation times or the signal intensities of the pixels, measured at different echo times in a multi-echo experiment. The observations are divided into clusters so that each pixel belongs to one cluster (tissue class or tissue subclass). After multiplication by pixel size the cluster areas (fat and muscle areas) can be used as regressors in a multiple regression analysis to derive prediction equations, or, if they are already available, to predict lean and fat content (Scholz et al., 1993; Baulain, 1997). An additional multiplication with slice thickness will provide a volume measure. A cross-validation should always be performed when using prediction equations. However, direct measures of body composition components, such as MRI volumes, are more accurate than indirect or estimated measures (Guo et al., 1996).

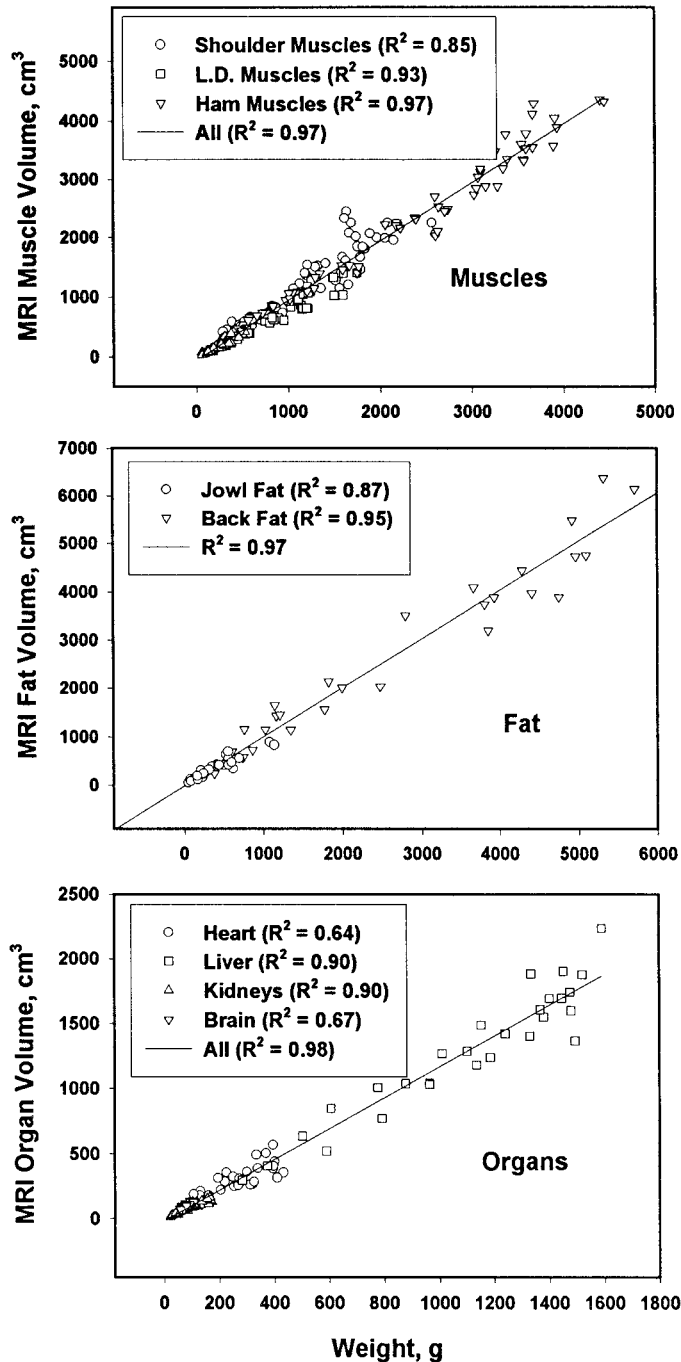


Figure 5. Relationship between dissected weights and magnetic resonance imaging (MRI) volumes of muscles (top), fat regions (middle), and internal organs (bottom) of pigs ranging in weight from 8.5 to 60.5 kg (Exp. 1).

**Table 2.** Comparison of various magnetic resonance imaging (MRI) tissue volume measurements for predicting total body fat, lean, or protein content of pigs from Exp. 2<sup>a</sup> (R<sup>2</sup> and SEE)<sup>b</sup>

Measurement	R <sup>2</sup> (SEE)		R <sup>2</sup> (SEE)		R <sup>2</sup> (SEE)	
	Fat, %		Lean, %		Protein, %	
Tissue volume, % <sup>c</sup>						
Jowl fat	0.046	(3.54)	0.088	(3.70)	0.009	(0.67)
Back fat	0.783*	(1.69)	0.725*	(2.03)	0.095	(0.64)
Shoulder muscle	0.026	(3.57)	0.109	(3.66)	0.186*	(0.61)
Longissimus muscle	0.161	(3.32)	0.0001	(3.88)	0.194*	(0.61)
Psoas muscle	0.006	(3.61)	0.133	(3.61)	0.109	(0.64)
Ham muscle	0.134	(3.37)	0.017	(3.85)	0.165	(0.62)
Fat:muscle ratio	0.489*	(2.59)	0.624*	(2.38)	0.224*	(0.60)
Tissue volume, cm <sup>3</sup>						
Jowl fat	0.550*	(2,460)	0.537*	(7,711)	0.407*	(1,875)
Back fat	0.952*	(803)	0.832*	(4,637)	0.708*	(1,315)
Shoulder muscle	0.859*	(1,375)	0.981*	(1,555)	0.915*	(711)
Longissimus muscle	0.809*	(1,600)	0.964*	(2,151)	0.939*	(599)
Psoas muscle	0.693*	(2,032)	0.860*	(4,239)	0.888*	(815)
Ham muscle	0.916*	(1,064)	0.982*	(1,511)	0.903*	(757)
Fat:muscle ratio	0.156	(3,369)	0.048	(11,120)	0.048	(2,423)

<sup>a</sup>Male and female pigs, 10 to 60 kg, n = 22.

<sup>b</sup>R<sup>2</sup> values followed by \* are statistically significant at  $P < 0.05$  ( $F$ -test); SEE = standard error of estimate.

<sup>c</sup>Tissue volume, % = MRI volume (cm<sup>3</sup>)/100 g BW.

Generally, it can be stated that the reproducibility of subcutaneous fat area measurements on MR images using image analysis software is higher than it is for visceral fat areas (coefficient of variations < 5.0% vs > 9.0% to 26%). The visceral fat depot is more subject to measurement errors due to operator and software misclassifications of pixels caused by movement artifacts, magnetic field inhomogeneities, and partial volume effects. Consequently, CT may be more accurate than MRI for measuring visceral fat volume (Seidell et al., 1990). In swine, subcutaneous fat content can be determined with a slightly higher accuracy than lean (meat) content. The use of several measuring positions will increase accuracy for some traits. A knowledge-based image processing (definition of regions of interest) procedure with options for a correction of automatically defined regions of interest is the best choice for an accurate and reproducible MRI analysis of body composition. An objective statistical image analysis is based on the signal intensity distribution (gray value distribution) for each single slice and relies on an "artifact-free" MR-image acquisition. Exact volume measurements provide a direct measure of body composition and should be preferred over an estimation of body composition using regression equations with a high number of image variables (Baulain, 1997; Elbers et al., 1997; Mitchell and Scholz, 2000).

In human studies a variety of image analysis techniques have been used. For example, Morais et al. (2000) used a combination of edge detection and watershed algorithm techniques to measure abdominal and thoracic adipose and lean volumes, Lee et al. (2000) used either a threshold based on an adipose and lean

gray-level histogram or a filter-based watershed algorithm to measure total body skeletal mass, Fuller et al. (1999) used region growing techniques to measure limb muscle and adipose tissue volume, and Engelson et al. (1999) manually identified and quantified visceral adipose and lean tissue compartments.

Fowler et al. (1992) found that MRI-measured adipose volumes accurately quantified the percentage of adipose tissue in pigs compared with either dissection or chemical analysis. Results of volume analysis by MRI were in excellent agreement with dissection for measuring differences in fat, muscle, and organ sizes as the result of growth hormone treatment in pigs (Mitchell et al., 1991b). Kallweit et al. (1994) reported coefficients of determination (R<sup>2</sup>) ranging from 0.48 to 0.93 for the estimation of absolute amounts and proportions of fat and lean tissues among three weight groups of pigs.

In analyzing adipose tissue from 13 locations along the body of the pig, Fowler et al. (1992) found that MRI measurements correlated with dissection ( $r = 0.98$ ) and chemical analysis ( $r = 0.98$ ). Baulain et al. (1998) scanned and then dissected pork belly cuts from Pietrain, German Landrace, and Pietrain  $\times$  German Landrace. For the three breeds of pigs, the correlation between lean content determined by imaging and dissection ranged from 0.72 to 0.94. A study by Kastelic et al. (1996) used MRI volume measurements of pigs at 20, 35, 50, and 70 kg to determine the allometric growth of muscles and fat areas.

Relating MRI volume measurements of muscle and adipose tissue to dissection or chemical analysis involves certain assumptions. In general, the hydration status of both muscle and adipose tissue can vary with

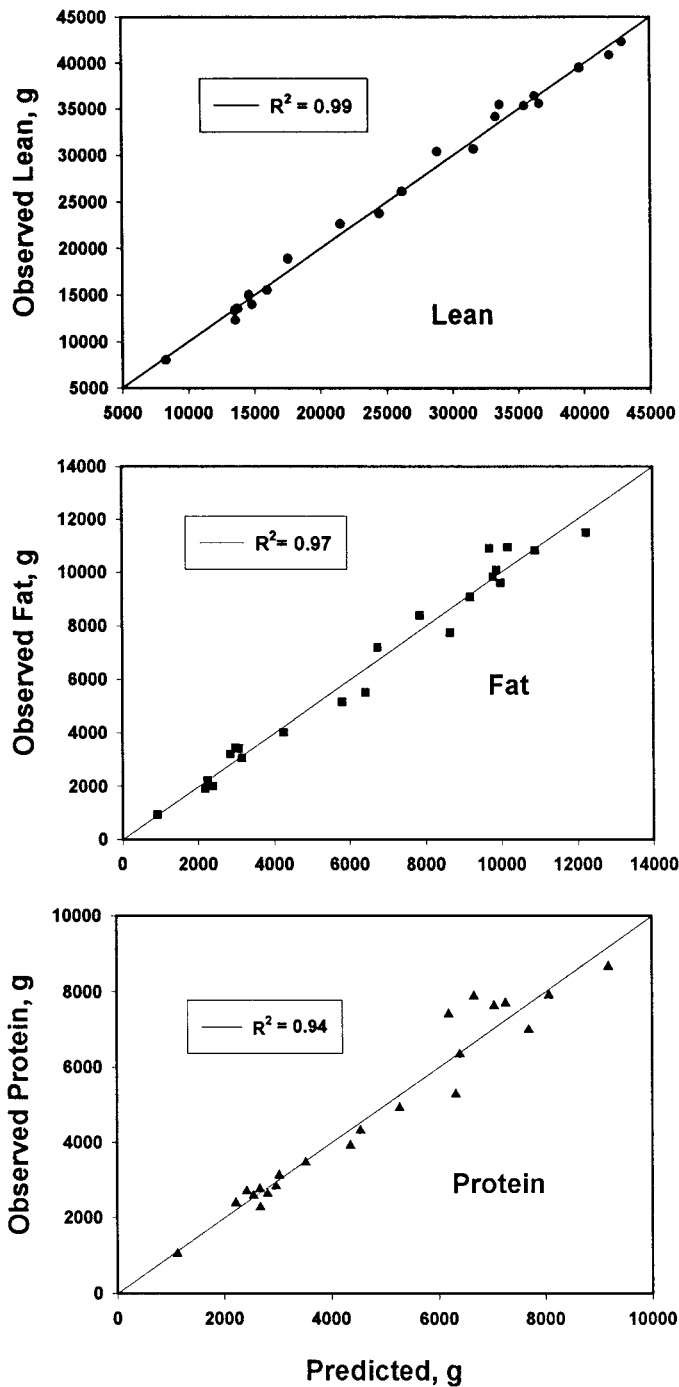


**Figure 6.** Relationship between observed fat, lean, and protein content of pigs and the amounts predicted from multiple regression equations using magnetic resonance imaging (MRI) volume measurements of fat and muscle areas (10 to 60 kg BW,  $n = 22$ , Exp. 2). The prediction equations were as follows: Lean (g) =  $4,331 + 0.906 \times \text{BF} + 3.294 \times \text{SM} + 4.511 \times \text{LDM}$ ; Fat (g) =  $-231.4 - 1.252 \times \text{JF} + 1.38 \times \text{BF} + 0.96 \times \text{SM}$ ; Protein (g) =  $240.6 - 1.221 \times \text{JF} + 0.257 \times \text{BF} + 0.927 \times \text{SM} + 10.367 \times \text{PM}$ , where the MRI volumes of jowl fat (JF), backfat (BF), shoulder muscle (SM), longissimus muscle (LDM), and psoas muscle (PM) are expressed as cubic centimeters.

age, disease, or hormonal status, although only under severe conditions would volume be altered significantly. Because of the correlation between the length of the  $T_1$  relaxation time and free tissue water (Bottomley et al., 1984), an increase in the hydration of either muscle or adipose tissue results in an increase in the maximum  $T_1$  relaxation time (Møller et al., 1994). This can be determined by MR spectroscopy of the tissues. In the measurement of subcutaneous adipose tissue, there is not a distinct boundary between the adipose tissue and the overlying skin, and thus the skin is usually included with the measurement of the adipose tissue. The presence of intramuscular fat can be quantified by MR spectroscopic procedures (Geers et al., 1995) but cannot be easily excluded from MRI volume measurements and is, therefore, included in the muscle measurements. However, deposits of intermuscular fat can be distinguished (depending on size) and excluded from the measurement. Although the data reported in the present study directly compare MRI volume to tissue weights (which assumes a tissue density of 1.0), tissue mass and volume are more precisely interconverted using an assumed density of 1.04 kg/L for muscle and 0.916 kg/L for adipose tissue (Fuller et al., 1999).

Although other imaging techniques, such as CT and in some cases ultrasound, can be used for measurements of fat and muscle regions, MRI is far superior for volumetric analysis of the internal organs. In this study, some tissue or blood loss occurred in dissecting the brain and heart, particularly the heart, which had become engorged with blood following the lethal dose of pentobarbital. In general, volume measurements of the internal organs could have been improved by decreasing the slice thickness, thus increasing the number of slices (Elliott et al., 1997).

It is difficult to obtain accurate volumetric analysis of smaller tissues and organs from a total body scan. The problem lies in the relationship between size of the tissue or organ and the slice thickness. This was illustrated for volumetric analysis of the pectoral muscle of the chicken (Mitchell et al., 1991c). Also, image resolution is determined by slice thickness and the in-plane pixel size. When the slice is thick relative to the size of the tissue, the circumference of the tissue can change from one edge of the slice to the next, resulting in an image that is fuzzy and impossible to trace accurately. These relationships, also known as partial volume effects, may be responsible for the consistent difference between the MRI volumes and dissected weights of the longissimus and psoas muscles. Elliott et al. (1997) found that the largest source of error in MRI volume measurements was due to partial volume effects, which resulted in overestimation of phantom volumes ranging from 145 to 900 mL by 6 to 13%. They also showed that the magnitude of this effect increased with decreasing object size and decreasing spatial resolution. Therefore, if there is a particular tissue or organ that is of interest, the slice selection parameters need to be tailored to that specific region (Manning et al., 1990; Fowler et al.,

**Table 3.** Comparison of various magnetic resonance image (MRI) volume measurements of 10-cm sections of both longissimus muscles and their overlying fat (Exp. 3, 26 to 97 kg, n = 46; Exp. 4, 6.1 to 15 kg, n = 15; Exp. 3 + 4, n = 61) and 15-cm sections of ham lean tissue and overlying fat (Exp. 3) for predicting the fat content of pigs (R<sup>2</sup> and SEE)<sup>a</sup>

Measurement	Exp. 3		Exp. 4		Exp. 3 + 4	
	R <sup>2</sup>	(SEE)	R <sup>2</sup>	(SEE)	R <sup>2</sup>	(SEE)
Fat, %						
Tissue volume, cm <sup>3</sup>						
Longissimus muscle	0.260*	(4.08)	0.023	(2.06)	0.556*	(3.94)
Longissimus muscle, cm <sup>3</sup> /kg BW	0.190*	(4.02)	0.066	(2.02)	0.470*	(4.31)
Longissimus fat	0.866*	(1.74)	0.449*	(1.55)	0.892*	(2.05)
Longissimus fat, cm <sup>3</sup> /kg BW	0.657*	(2.85)	0.501*	(1.48)	0.548*	(4.25)
Longissimus fat/muscle	0.640*	(2.85)	0.639*	(1.25)	0.373*	(4.68)
Ham lean	0.412*	(3.64)				
Ham lean, cm <sup>3</sup> /kg BW	0.558*	(3.15)				
Ham fat	0.786*	(2.20)				
Ham fat, cm <sup>3</sup> /kg BW	0.011	(4.72)				
Ham fat/lean	0.264*	(4.07)				
Fat, g						
Tissue volume, cm <sup>3</sup>						
Longissimus muscle	0.602*	(3.83)	0.635*	(0.19)	0.765*	(3.43)
Longissimus fat	0.886*	(2.30)	0.806*	(0.14)	0.918*	(2.03)
Longissimus fat/muscle	0.321*	(5.26)	0.101	(0.30)	0.210*	(6.29)
Ham lean tissue	0.784*	(2.74)				
Ham fat	0.898*	(2.18)				
Ham fat/lean	0.038	(6.17)				

<sup>a</sup>R<sup>2</sup> followed by \* are significant at  $P < 0.05$  ( $F$ -test); SEE = standard error of estimate.

**Table 4.** Comparison of various magnetic resonance image (MRI) volume measurements of 10-cm sections of both longissimus muscles and their overlying fat (Exp. 3, 26 to 97 kg, n = 46; Exp. 4, 6.1 to 15 kg, n = 15; Exp. 3 + 4, n = 61) and 15-cm sections of ham lean tissue and overlying fat (Exp. 3) for predicting the lean content of pigs (R<sup>2</sup> and SEE)<sup>a</sup>

Measurement	Exp. 3		Exp. 4		Exp. 3 + 4	
	R <sup>2</sup>	(SEE)	R <sup>2</sup>	(SEE)	R <sup>2</sup>	(SEE)
Lean, %						
Tissue volume, cm <sup>3</sup>						
Longissimus muscle	0.256*	(3.75)	0.019	(2.49)	0.564*	(3.85)
Longissimus muscle, cm <sup>3</sup> /kg BW	0.214*	(3.85)	0.072	(2.42)	0.505*	(4.10)
Longissimus fat	0.827*	(1.81)	0.377*	(1.98)	0.849*	(2.39)
Longissimus fat, cm <sup>3</sup> /kg BW	0.596*	(2.76)	0.415*	(1.92)	0.480*	(4.20)
Longissimus fat/muscle	0.599*	(2.75)	0.566*	(1.65)	0.316*	(4.82)
Ham lean	0.408*	(3.34)				
Ham lean, cm <sup>3</sup> /kg BW	0.640*	(2.61)				
Ham fat	0.766*	(2.10)				
Ham fat, cm <sup>3</sup> /kg BW	0.005	(4.33)				
Ham fat/lean	0.255*	(3.75)				
Lean, g						
Tissue volume, cm <sup>3</sup>						
Longissimus muscle	0.850*	(5.31)	0.855*	(0.62)	0.920*	(5.06)
Longissimus fat	0.603*	(8.51)	0.515*	(1.14)	0.726*	(9.36)
Longissimus fat/muscle	0.071	(13.25)	0.007	(1.63)	0.047	(17.46)
Ham lean tissue	0.979*	(1.99)				
Ham fat	0.726*	(7.22)				
Ham fat/lean	0.016	(13.69)				

<sup>a</sup>R<sup>2</sup> followed by \* are significant at  $P < 0.05$  ( $F$ -test); SEE = standard error of estimate.

**Table 5.** Comparison of various magnetic resonance image (MRI) volume measurements of 10-cm sections of both longissimus muscles and their overlying fat (Exp. 3, 26 to 97 kg, n = 46; Exp. 4, 6.1 to 15 kg, n = 15; Exp. 3 + 4, n = 61) and 15-cm sections of ham lean tissue and overlying fat (Exp. 3) for predicting the protein content of pigs ( $R^2$  and SEE)<sup>a</sup>

Measurement	Exp. 3		Exp. 4		Exp. 3 + 4	
	$R^2$	(SEE)	$R^2$	(SEE)	$R^2$	(SEE)
Protein, %						
Tissue volume, cm <sup>3</sup>						
Longissimus muscle	0.007	(1.47)	0.001	(1.76)	0.060	(1.62)
Longissimus muscle, cm <sup>3</sup> /kg BW	0.084	(1.42)	0.187	(1.58)	0.003	(1.67)
Longissimus fat	0.204*	(1.32)	0.183	(1.59)	0.000	(1.67)
Longissimus fat, cm <sup>3</sup> /kg BW	0.230*	(1.30)	0.144	(1.63)	0.077	(1.60)
Longissimus fat/muscle	0.253*	(1.28)	0.369*	(1.40)	0.175	(1.52)
Ham lean	0.033	(1.46)				
Ham lean, cm <sup>3</sup> /kg BW	0.232*	(0.81)				
Ham fat	0.177*	(1.34)				
Ham fat, cm <sup>3</sup> /kg BW	0.074	(1.43)				
Ham fat/lean	0.184*	(1.34)				
Protein, g						
Tissue volume, cm <sup>3</sup>						
Longissimus muscle	0.832*	(1.41)	0.864*	(0.12)	0.911*	(1.31)
Longissimus fat	0.584*	(2.22)	0.341*	(0.26)	0.715*	(2.35)
Longissimus fat/muscle	0.067	(3.32)	0.062	(0.32)	0.045	(4.29)
Ham lean tissue	0.944*	(0.81)				
Ham fat	0.677*	(1.95)				
Ham fat/lean	0.022	(3.40)				

<sup>a</sup> $R^2$  followed by \* are significant at  $P < 0.05$  ( $F$ -test); SEE = standard error of estimate.

1991; Scollan et al., 1998). For small subjects or small regions within the body, the MR spectroscopic signal (amplitude or area of the water and lipid proton signals)

can be used to measure the relative content of fat and lean tissue (Stelwaagen et al., 1990; Mitchell et al., 1991a; Lirette et al., 1993).

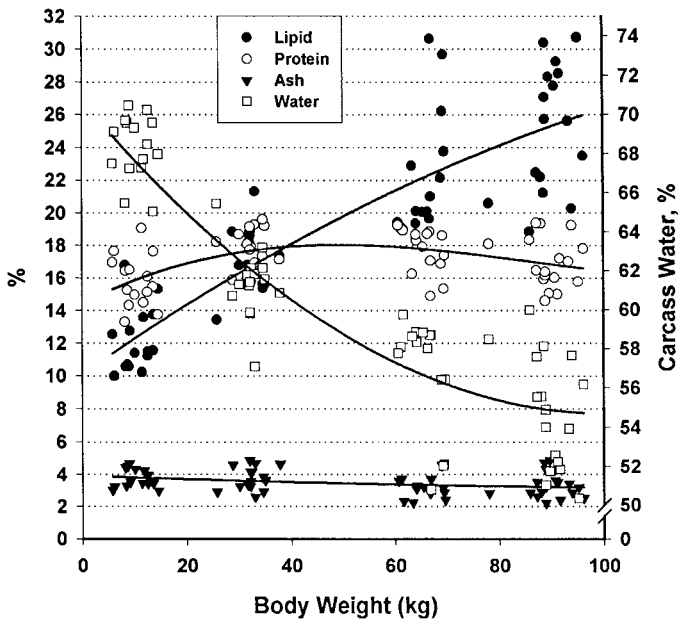


**Figure 7.** Development of the carcass composition of male and female pigs, based on the chemical analysis of 61 pigs at weights ranging from 6 to 97 kg (Exp. 3 and 4).

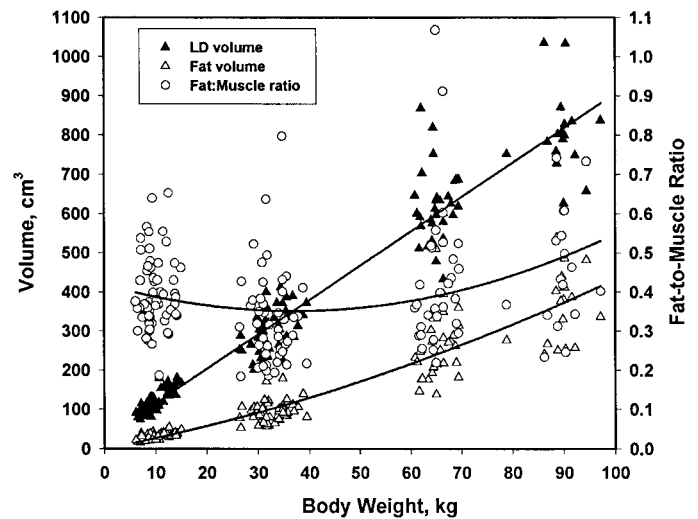


**Figure 8.** Relationship between body weight of live male and female pigs and magnetic resonance imaging (MRI) measurements of the volumes of the longissimus muscle (LD volume), overlying fat (Fat volume), and the fat:muscle ratio of the same regions (6 to 97 kg BW, n = 61, Exp. 3 and 4).

**Table 6.** Models selected for prediction of body composition of pigs using magnetic resonance image (MRI) volume measurements of fat and muscle regions

Variable	R <sup>2</sup>	SEE <sup>a</sup>	Parameters in equation <sup>b</sup>
Carcass lipid %			
Exp. 2 <sup>c</sup>	0.83	1.546	J fat vol%, B fat vol%, LD muscle vol%
Exp 3 <sup>d</sup>	0.90	1.500	LD fat vol, H fat:muscle ratio
Exp. 4 <sup>e</sup>	0.64	1.253	LD fat:muscle ratio
Exp 3 + 4 <sup>f</sup>	0.91	1.761	LD fat vol, LD muscle vol%
Carcass protein %			
Exp. 2	0.62	0.46	J fat vol%, B fat vol%, SH muscle vol%, H muscle%, Fat:muscle ratio
Exp. 3	0.25	1.280	LD fat:muscle ratio
Exp. 4	0.37	1.396	LD fat:muscle ratio
Exp. 3 + 4	0.27	1.442	LD fat vol, LD fat:muscle ratio
Carcass lean %			
Exp. 2	0.76	1.834	B fat vol%, LD muscle vol%, Fat:muscle ratio
Exp. 3	0.88	1.539	LD fat vol, H fat:muscle ratio, H lean vol%
Exp. 4	0.57	1.654	LD fat:muscle ratio
Exp 3 + 4	0.89	1.984	LD fat vol, LD muscle vol%

<sup>a</sup>Standard error of estimate.

<sup>b</sup>Abbreviations used: J = jowl, B = back, LD = longissimus muscle, H = ham, SH = shoulder, vol = volume (cm<sup>3</sup>), vol% = volume as a percentage of total body weight.

<sup>c</sup>Exp. 2: 10 to 60 kg, n = 22.

<sup>d</sup>Exp. 3: 26 to 97 kg, n = 46.

<sup>e</sup>Exp. 4: 6 to 15 kg, n = 15.

<sup>f</sup>Exp. 3 + 4: 6 to 97 kg, n = 61.

For the prediction of total body composition from MRI analysis, a number of approaches are possible. The highest accuracy, defined as a measure of the performance of a prediction equation applied to an independent sample, would result from whole-body analysis (Guo et al., 1996). Using rats, Ross et al. (1991) performed total body scans and found that MRI accurately measured visceral, subcutaneous, and total adipose tissue content. Engelson et al. (1999) used total body MRI image analysis to measure total body skeletal muscle and fat and fat distribution in human subjects. Likewise, total body image analysis is possible with pigs but is not practical for most research studies. Total body image acquisition can be accomplished within a reasonable time frame (approximately 12 min per 40 1-cm slices). The MR image results in a wide range of pixel intensities, making automated analysis difficult. This is especially true of total body imaging of a large subject; due to inhomogeneity of the radio frequency and magnetic fields, there can be a wide range of intensities for the same type of tissue at different locations within an individual slice.

An alternative is to predict total body composition based on analysis of specific regions, either selected tissue regions as in Exp. 2 of this study or selected slices from different areas of the body as in Exp. 3 and 4 of this study. In the study by Fowler et al. (1992), in which 13 slices at locations throughout the length of the body of 12 pigs were analyzed for fat content, MRI closely predicted percentage of total body adipose tissue (R<sup>2</sup> = 0.98). Accuracy decreased only slightly if only two sections were used. Baulain et al. (1996) analyzed slices from five body regions of 143 pigs and reported R<sup>2</sup> ≥ 0.9

for total fat and lean and R<sup>2</sup> ≥ 0.8 for percentages of fat and lean.

Comparing the results of Exp. 2, 3, 4, and 3 + 4, the most accurate prediction of fat and lean content was obtained by analyzing the fat and muscle values of a specified number of slices within the ham and loin regions (Exp. 3 and 4). This suggests that a precise measurement of the fat and muscle volumes within a well-defined area of the loin and ham regions is of more value for predicting the percentages of fat and lean in the total body than is the total volume of either fat or muscle of a less-well-defined region. However, results from Exp. 2 indicate that protein content was more accurately predicted using fat and muscle volumes from several regions (jowl fat, back fat, shoulder muscle, and ham muscle volumes). Typically, protein content is highly correlated with muscle or lean (lean = water + protein); however, percentage of protein can be influenced by total fat, intramuscular fat, tissue hydration, and, in the case of total body analysis, the contribution of internal organs. Thus, total body protein content is more difficult to predict and may require more extensive information in order to obtain a higher correlation.

## Implications

Magnetic resonance imaging offers a number of possibilities for noninvasive in vivo body composition analysis of the pig, ranging from volumetric measurement of a specific tissue or organ to prediction of total body fat and lean content. Based on image analysis of total body scans, better agreement between image volume and dissection weight was obtained for larger organs and

tissues, suggesting that the accuracy of volumetric analysis may depend on the relationship between slice thickness and tissue size. Volume measurements of the fat and muscle from well-defined regions of the back and ham regions provide information for the accurate prediction of total body composition of the pig.

### Literature Cited

- Baulain, U. 1997. Magnetic resonance imaging for the in vivo determination of body composition in animal science. *Comput. Electron. Agric.* 17:189–203.
- Baulain, U., M. Henning, and E. Kallweit. 1996. Bestimmung der Körperzusammensetzung von Landrasse-Schweinen unterschiedlichen Alters mittels MRI. [Determination of body composition in German Landrace pigs of various ages by means of MRI]. *Arch. Tierz.* 39:431–440.
- Baulain, U., M. Henning, E. Tholen, W. Whittmann, and W. Peschke. 1998. Objective methods for estimation of the lean meat content of pig belly. 2. Use of scans from magnetic resonance imaging. *Züchtungskunde* 70:205–212.
- Baulain, U., and A. Scholz. 1996. Image evaluation for different acquisition techniques in animal production. In: *Proc. 47th Annu. Mtg. Europ. Assoc. Anim. Prod., Lillehammer, Norway.* p 269. (Abstr.).
- Borrello, J. A., T. L. Chenevert, C. R. Meyer, A. M. Aisen, and G. M. Glazer. 1987. Chemical shift-based true water and fat images: Regional phase correction of modified spin-echo MR images. *Radiology* 164:531–537.
- Bottomley, P. A., T. H. Foster, R. E. Argersinger, and L. M. Peifer. 1984. A review of normal tissue hydrogen NMR relaxation time and relaxation mechanisms from 1–100 MHz: Dependence on tissue type, NMR frequency, temperature, species, excision, and age. *Med. Phys. (NY)* 11:425–448.
- Elbers, J. M. H., G. Haumann, H. Asscheman, J. C. Seidell, and L. J. G. Gooren. 1997. Reproducibility of fat area measurements in young, non-obese subjects by computerized analysis of magnetic resonance images. *Int. J. Obes.* 21:1121–1129.
- Elliott, M. A., G. A. Walter, H. Gulish, A. S. Sadi, D. D. Lawson, W. Jaffe, E. K. Insko, J. S. Leigh, and K. Vandeborne. 1997. Volumetric measurement of human calf muscle from magnetic resonance imaging. *MAGMA* 5:93–98.
- Engelson, E. S., D. P. Kotler, Y. X. Tan, D. Agin, J. Wang, R. N. Pierson, and S. B. Heymsfield. 1999. Fat distribution in HIV-infected patients reporting truncal enlargement quantified by whole-body magnetic resonance imaging. *Am. J. Clin. Nutr.* 69:1162–1169.
- Folch, J. M., M. Lees, and G. H. Sloan-Stanley. 1957. A simple method for the isolation and purification of total lipids from animal tissues. *J. Biol. Chem.* 226:497–509.
- Foster, M. A., and P. A. Fowler. 1988. Noninvasive methods for assessment of body composition. *Proc. Nutr. Soc.* 47:375–385.
- Fowler, P. A., M. F. Fuller, C. A. Glasbey, G. G. Cameron, and M. A. Foster. 1992. Validation of the in vivo measurement of adipose tissue by magnetic resonance imaging of lean and obese pigs. *Am. J. Clin. Nutr.* 56:7–13.
- Fowler, P. A., C. H. Knight, and M. A. Foster. 1991. In-vivo magnetic resonance imaging studies of mammogenesis in non-pregnant goats treated with exogenous steroids. *J. Dairy. Res.* 58:151–157.
- Fuller, M. F., P. A. Fowler, G. McNeill, and M. A. Foster. 1994. Imaging techniques for the assessment of body composition. *J. Nutr.* 124:1546S–1550S.
- Fuller, N. J., C. R. Haardingham, M. Graves, N. Sreaton, A. K. Dixon, L. C. Ward, and M. Elia. 1999. Assessment of limb muscle and adipose tissue by dual-energy X-ray absorptiometry using magnetic resonance imaging for comparison. *Int. J. Obes.* 23:1295–1302.
- Fuller, M. F., S. M. Stratton, D. Geddes, P. A. Fowler, and M. A. Foster. 1987. A study of the sites of adipose tissue loss by NMR imaging. In: K. J. Ellis, S. Yasumura, and W. D. Morgan (ed.) *In Vivo Body Composition Studies.* pp 55–59. The Institute of Physical Sciences in Medicine, London.
- Geers, R., C. Decanniere, H. Villé, P. Van Hecke, and L. Bosschaerts. 1995. Variability within intramuscular fat content of pigs as measured by gravimetry, FTIR and NMR spectroscopy. *Meat Sci.* 40:373–378.
- Glover, G. H., and E. Schneider. 1991. Three-point Dixon technique for true water/fat decomposition with B0 inhomogeneity correction. *Magn. Reson. Med.* 18:371–383.
- Guo, S. S., W. C. Chumlea, and D. B. Cockram. 1996. Use of statistical methods to estimate body composition. *Am. J. Clin. Nutr.* 64:428S.
- Heymsfield, S. B., R. Ross, Z. Wang, and D. Frager. 1997. Imaging techniques of body composition: Advantages of measurement and new uses. In: S. J. Carlson-Newberry and R. B. Costello (ed.) *Emerging Technologies for Nutrition Research: Potential for Assessing Military Performance Capability.* pp 127–150. National Academy Press, Washington, DC.
- Kaldoudi, E., and S. C. R. Williams. 1992. Fat and water differentiation by nuclear magnetic resonance imaging. *Concepts in Magn. Reson.* 4:53–71.
- Kallweit, E., H. H. Wesemeier, D. Smidt, and U. Baulain. 1994. Einsatz der Magnet-Resonanz-Messung in der Tierzuchtforschung. [Application of Magnetic Resonance-Measurements in Animal Research]. *Arch. Tierz.* 37:105–120.
- Kastelic, M., U. Baulain, and E. Kallweit. 1996. Allometric growth of muscle and fat areas in German Landrace pigs. In: *Proc. 47th Annu. Mtg. Europ. Assoc. Anim. Prod., Lillehammer, Norway.* p 279 (Abstr.).
- Lee, R. C., Z. M. Wang, M. Heo, R. Ross, I. Janssen, and S. B. Heymsfield. 2000. Total-body skeletal muscle mass: Development and cross-validation of anthropometric prediction models. *Am. J. Clin. Nutr.* 72:796–803.
- Lirette, A., R. A. Towner, Z. Liu, E. G. Janzen, J. R. Chambers, R. W. Fairfull, L. P. Milligan, and D. C. Crober. 1993. In vivo nuclear magnetic resonance spectroscopy of chicken embryos from two broiler strains of varying fat content. *Poult. Sci.* 72:1411–1420.
- Luiting, P., K. Kolstad, H. Enting, and O. Vangen. 1995. Pig breed comparison for body composition at maintenance: Analysis of computerized tomography data by mixture distributions. *Livest. Prod. Sci.* 43:225–234.
- Manning, W. J., J. Y. Wei, E. T. Fossel, and D. Burstein. 1990. Measurement of left ventricular mass in rats using electrocardiogram-gated magnetic resonance imaging. *Am. J. Physiol.* 258:H1181–1186.
- Mitchell, A. D., and A. M. Scholz. 2000. Techniques for measuring body composition of swine. In: A. J. Lewis (ed.) *Swine Nutrition.* 2nd ed. pp 915–958. CRC Press, Boca Raton, FL.
- Mitchell, A. D., P. C. Wang, and T. H. Elsasser. 1991a. Determination of fat and water content in vitro and in vivo by proton nuclear magnetic resonance. *J. Sci. Food Agric.* 56:265–276.
- Mitchell, A. D., P. C. Wang, T. H. Elsasser, and W. F. Schmidt. 1991b. Application of NMR spectroscopy and imaging for body composition analysis as related to sequential measurement of energy deposition. In: C. Wenk and M. Boessinger (ed.) *Energy Metabolism of Farm Animals.* pp 222–225. Europ. Assoc. Anim. Prod. Publ. No. 58.
- Mitchell, A. D., P. C. Wang, R. W. Rosebrough, T. H. Elsasser, and W. F. Schmidt. 1991c. Assessment of body composition of poultry by nuclear magnetic resonance imaging and spectroscopy. *Poult. Sci.* 70:2494–2500.
- Møller, J., J. O. L. Jørgensen, N. Møller, H. Stødkilde-Jørgensen, and J. S. Christiansen. 1994. Assessment of fat and muscle volume and water content by magnetic resonance imaging (MRI) and proton spectroscopy in growth hormone (GH) deficient adults before and after GH treatment. *Endocrinol. Metab.* 1:131–135.
- Morais, J. A., R. Ross, R. Gougeon, P. B. Pencharz, P. J. H. Jones, and E. B. Marliss. 2000. Distribution of protein turnover changes with age in humans as assessed by whole-body magnetic reso-

- nance image analysis to quantify tissue volumes. *J. Nutr.* 130:784–791.
- Ross, R., L. Leger, R. Guardo, J. De Guise, and B. G. Pike. 1991. Adipose tissue volume measured by magnetic resonance imaging and computerized tomography in rats. *J. Appl. Physiol.* 70:2164–2172.
- Scholz, A., U. Baulain, and E. Kallweit. 1993. Quantitative Analyse von Schnittbildern lebender Schweine aus der Magnet-Resonanz-Tomographie. [Multivariate statistical analysis of images from magnetic resonance tomography on living pigs.] *Züchtungskunde* 65:206–215.
- Scholz, A. M., A. D. Mitchell, P. C. Wang, H. Song, and Z. Yan. 1995. Muscle metabolism and body composition of pigs with different ryanodine receptor genotypes studied by means of  $^{31}\text{P}$  nuclear magnetic resonance spectroscopy and  $^1\text{H}$  magnetic resonance imaging. *Arch. Tierz.* 38:539–552.
- Scollan, N. D., L. J. Caston, Z. Liu, A. K. Zubair, S. Leeson, and B. W. McBride. 1998. Nuclear magnetic resonance imaging as a tool to estimate the mass of the pectoralis muscle of chickens in vivo. *Br. Poult. Sci.* 39:221–224.
- Seidell, J. C., C. J. G. Bakker, and K. Kooy. 1990. Imaging techniques for measuring adipose-tissue distribution—a comparison between computed tomography and 1.5-T magnetic resonance. *Am. J. Clin. Nutr.* 51:953–957.
- Stark, D. D., and W. G. Bradley, Jr. 1999. *Magnetic Resonance Imaging*. 3rd ed. Mosby, St. Louis, MO.
- Stelwaagen, K., B. W. McBride, D. G. Grieve, and T. A. Towner. 1990. Nuclear magnetic resonance imaging and proton spectroscopy used as a technique to assess mammary gland composition in Holstein heifers. *Can. J. Anim. Sci.* 70:1151–1154.
- Szabo, C., L. Babinszky, M. W. A. Verstegen, O. Vangen, A. J. M. Jansman, and E. Kanis. 1999. The application of digital imaging techniques in the in vivo estimation of the body composition of pigs: A review. *Livest. Prod. Sci.* 60:1–11.
- Tang, H., J. Vasselli, E. Wu, and D. Gallagher. 2000. In vivo determination of body composition of rats using magnetic resonance imaging. *Ann. N.Y. Acad. Sci.* 904:32–41.
- Thomas, E. L., N. Saeed, J. V. Hajnal, A. Brynes, A. P. Goldstone, G. Frost, and J. D. Bell. 1998. Magnetic resonance imaging of total body fat. *J. Appl. Physiol.* 85:1778–1785.
- Yeung, H. N., and D. W. Kormos. 1986. Separation of true fat and water images by correcting magnetic field inhomogeneity in situ. *Radiology* 159:783–786.